Colloids and Surfaces A: Physicochem. Eng. Aspects 460 (2014) 225–235

Contents lists available at ScienceDirect

Colloids and Surfaces A: Physicochemical and Engineering Aspects

journal homepage: www.elsevier.com/locate/colsurfa

Nanoprecipitation of polymers in a bad solvent

J.G.J.L. Lebouille[a], R. Stepanyan[b], J.J.M. Slot[b,c], M.A. Cohen Stuart[d], R. Tuinier[a,e,*]

[a] DSM ChemTech Center, Advanced Chemical Engineering Solutions (ACES), P.O. Box 18, 6160 MD Geleen, The Netherlands
[b] DSM Ahead, Materials Science Center, P.O. Box 18, 6160 MD Geleen, The Netherlands
[c] Department of Mathematics and Computer Science, Eindhoven University of Technology, P.O. Box 513, 5600 MB Eindhoven, The Netherlands
[d] Laboratory of Physical Chemistry and Colloid Science, Wageningen University, Dreijenplein 6, 6307 HB Wageningen, The Netherlands
[e] Van't Hoff Laboratory for Physical and Colloid Chemistry, Department of Chemistry, Utrecht University, Padualaan 8, 3584 CH Utrecht, The Netherlands

HIGHLIGHTS

- Nanoprecipitation of polymers in a bad solvent with surfactants was examined.
- We derived a kinetic model for diffusion limited coalescence.
- Final nanoparticle size is independent of polymer molar mass of the polymer.
- The final particle volume increases linearly with polymer concentration.
- Experimental results are in good agreement with theoretical predictions.

GRAPHICAL ABSTRACT

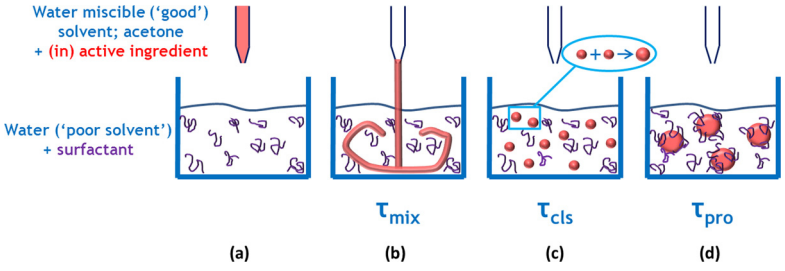

ARTICLE INFO

Article history:
Received 27 August 2013
Received in revised form
22 November 2013
Accepted 23 November 2013
Available online 1 December 2013

Keywords:
(Nano)Precipitation
Particle size
Encapsulation
Surfactant
Polymer
Diffusion limited coalescence

ABSTRACT

Nanoparticles (NPs) composed of polymers are of great interest since they can add a functionality in many applications, ranging from food and pharma to plastics and electronics. A key factor that determines the functionality of NPs is their size. Nanoprecipitation [1] is a commonly used technique to prepare NPs. We have performed a combined experimental and theoretical study on the size of NPs formed by precipitation of polymers into a bad solvent in the presence of a stabilizing surfactant.

We propose an extension of the theoretical framework put forward by Lannibois et al. [10] for nanoparticle formation via precipitation. Our theory is based upon a kinetic model for diffusion limited coalescence (DLC) in which the relevant transport and diffusion mechanisms are quantified. We find that the macroscopic mixing time and the diffusivity of the polymer and surfactant are the main parameters determining the final particle size. The theoretical result for the final size can be condensed into a single analytical expression. At given polymer concentration and mixing time, it follows that the smallest particles can be obtained in the excess of surfactant. This situation corresponds well to the experimentally used conditions. The mixing efficiency is predicted to have a profound influence on the final particle diameter: faster mixing results in smaller particles. The final particle size in the slow mixing regime, which is the typical situation in experiments, turns out to be independent of the molar mass of the polymer and scales as a power 1/3 with the initial polymer concentration. An increase of the surfactant molar mass is predicted to lead to larger particles, because of longer mixing time and lower surfactant mobility.

We have performed systematic experimental investigations on nanoparticles formation using various systems but focused on polycaprolactone (PCL) polymers in acetone precipitated in aqueous solutions

* Corresponding author. Tel.: +31 620148067.
E-mail address: remco.tuinier@dsm.com (R. Tuinier).

0927-7757/$ – see front matter
http://dx.doi.org/10.1016/j.colsurfa.2013.11.045

containing polyvinyl alcohol as surfactant. The PCL molar mass and concentration and mixing time were varied. We show that both our experimental results as well as literature data are in good agreement with our theoretical DLC predictions. This work therefore provides a solid framework for tailoring nanoparticles with a desired size.

1. Introduction

Nanoprecipitation [1,2] is a promising technique for encapsulating hydrophobic species in nanoparticles dispersed in aqueous systems [3,4]. Although the method itself is quite versatile and can be used for a broad range of hydrophobic polymers [5], until now it has mainly been applied for the preparation of poly-(lactic-co-glycolic) acid (PLGA) and polycaprolactone (PCL) particles for drug delivery. The main promise of the technique has been a possibility to encapsulate a hydrophobic drug in a submicron particle and thereby effectively increase its water solubility. For a short overview of applications in physics, medicine and chemistry, see [6–9].

A typical set up of a nanoprecipitation experiment is depicted in Fig. 1. Hydrophobic species (a polymer such as PLGA in this example and/or drug) are dissolved in acetone. Note that PLGA can be replaced with polymers such as PCL. At room temperature, the acetone solution is injected into an aqueous solution of (polymeric) surfactant such as polyvinyl alcohol (PVA). After some short period of time a suspension of submicron particles is obtained.

Although seemingly quite straightforward, applying the technique for practical applications is not free of difficulties. For drug delivery applications, the nanoparticles have to fulfill strict dimensional criteria and should be stable over sufficiently long times. Although some particular methods, such as nanoprecipitation, have been studied experimentally quite thoroughly, there is limited correlation with the underlying physics that determines the final particle size. A physical picture of the nanoprecipitation process of hydrophobic molecules in water and the role of stabilizing surfactants was described by Lannibois et al. [10], and was being extended to high concentrations of polymeric hydrophobic compounds [11] and applied to obtain rather narrow size distributions [12]. Knowledge of the physics that governs the nanoprecipitation process could help to rationalize how various experimental parameters, such as mixing efficiency/time, surfactant and polymer concentration and molar masses, affect the final particle size. This tremendously facilitates the design of a smarter preparation protocol.

For pharmaceutical applications a hydrophobic polymer (drug carrier) is typically used in combination with a polymeric surfactant to form water-suspendable particles. Alternatively, (di)block copolymers can be used that offer the advantage of a stronger interaction with the carrier polymer. A vast amount of research has been devoted to this topic, especially experimentally [13–16], see also the reviews [17,18]. Particle formation using nanoprecipitation has also been studied using computer simulations and numerical methods, see for instance [10,14,19–21], whereas a simple theoretical model with explicit analytical expressions or at least a computationally 'cheap' numerical model for the size is much more helpful in steering the experimental research. The final size of block copolymer micelles in water, that apparently approaches equilibrium after a solvent switch [22], can be predicted very well by equilibrium self-consistent field computations [23,24]. For the systems studied here dynamics however plays a role.

From an application point of view, the polymeric surfactant system is strongly preferable compared to using copolymers. Therefore it is key to develop insight into the processes that are operational during micellar precipitation in a polymer/surfactant suspension. Lannibois et al. [10] have made a first step in understanding the main physics of particle formation, by realizing that the competition between coalescence of hydrophobic material and adsorption of surfactants at the water–hydrophobic droplet interface governs the final size.

The goal of this work is to further quantify the relevant diffusion processes during nanoparticle formation. Although the realistic applications of the nanoparticles always involve at least three components – surfactant, carrier polymer, and drug – we restrict ourselves to a system without any drug present. The main question to be answered is 'what (process as well as polymer and surfactant) parameters determine the end size of the nanoparticles?' As an example, one can think of the mixing intensity and temperature as typical process parameters, and molar masses and concentrations of the components as typical system parameters, and how these determine the final result.

The outline of this manuscript is as follows. First, we introduce the theoretical approach that considers diffusion limited coalescence in a quenched polymer solution in a bad solvent. The aim of this part is to identify the relevant coalescence rate of polymer particles in the absence of any stabilization. Then, we proceed by incorporating the surfactant into the system and show that in the limit of strong polymer–surfactant interaction the system arrives at a kinetically frozen state, in which each polymer particle is surrounded by a surfactant corona. The size of the particles is shown to depend on the interplay between the particle coalescence and the surfactant adsorption rates. Secondly, we report our systematic experimental results and literature data on nanoprecipitation in the light of the proposed theoretical model. This is followed by discussions on the combined experimental and theoretical results followed by the conclusions.

2. Theoretical framework

In this section we formulate a theoretical model to describe the nanoprecipitation process. Our goal is to provide a simple analytical expression for the nanoparticle (NP) size as a function of the mixing intensity and the surfactant and polymer properties while accounting for the essential features of the process. For the sake of simplicity, we restrict ourselves to a bi-component system and consider the case that a dilute solution of a hydrophobic polymer is injected into a water/surfactant solution. Both polymers and surfactants are subject to Brownian motion. Solvent and water are assumed to be well miscible which implies that a rapid quench of the hydrophobic polymer in water takes place. The polymers are now dispersed in a bad solvent so they form collapsed spheres, and these polymer particles start to coalesce upon encounter, to form larger particles. Simultaneously, the surfactant molecules adsorb onto the surface of the newly formed polymeric particles. This adsorption progressively hampers the coalescence process; steric repulsion between the surfactants prevents coalescence. Adsorption finally fully stabilizes the individual polymer particles against further coalescence and a stable situation is reached. The NPs formed represent a system in a kinetically frozen state. Therefore the NP size will depend strongly on the system kinetics, which includes at least three processes:

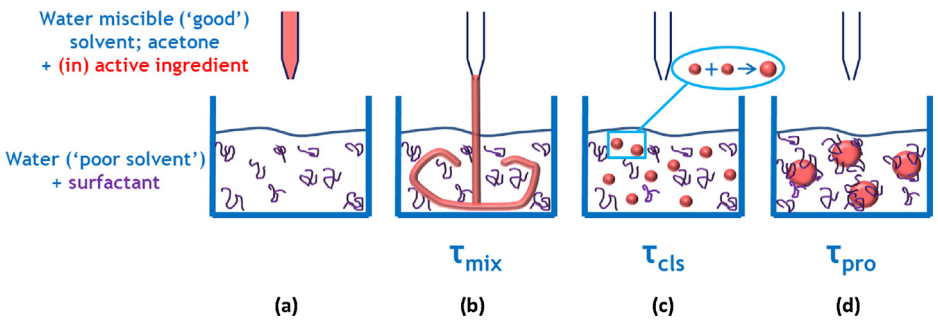

Fig. 1. Different stages of a nanoprecipitation experiment: (a) typically 1 mL of a 10 mg/mL PLGA or PCL solution in acetone is to be added to 10 mL of 1 wt% surfactant (for instance PVA or Pluronic F127) solution in water; (b) the macroscopic mixing step; (c) the initial state of the system considered: polymer spheres are homogeneously distributed within the experimental volume; (d) end of the experiment: polymer spheres have coalesced until a protective layer of surfactant (PVA or Pluronic F127) protects the individual spheres against coalescence.

- mixing polymer plus solvent with the aqueous surfactant solution on a time scale τ_{mix};
- coalescence of the hydrophobic polymer particles (nanodroplets) in a hostile water environment, characterized by a time scale τ_{cls} (we suppose that the collapsed polymer molecules represent a liquid rather than a solid state);
- protection of the polymeric NPs by surfactants on a time scale τ_{pro}. This last step brings the system into a kinetically frozen state.

Below we address these three processes in more detail. It is noted that a similar picture has been put forward in [10].

2.1. Diffusion limited coalescence in a polymer suspension

Before considering the process for the multicomponent system sketched in Fig. 1, let us address a somewhat simpler problem. Imagine a suspension of Brownian polymer particles (collapsed polymer chains) homogeneously distributed in a poor solvent. Such a situation actually corresponds to the limit of 'very fast mixing' or $\tau_{mix} \to 0$, i.e. a very rapid quench of a polymer solution. The initial situation is similar to the one depicted in Fig. 1(c) with one major difference – there is no surfactant. Apparently, in the course of time, the particles, subject to Brownian motion, will meet each other, collide and stick, forming larger particles. If they were hard (solid) particles, this would lead to fractal aggregates, for which well-known growth laws have been developed. This case is commonly known as 'diffusion limited aggregation' (DLA), leading to fractal clusters. Such an aggregation proceeds until the clusters meet and a space-spanning gel forms [25–27].

As our particles are liquid-like, they will coalesce to homogeneous spherical particles rather than forming fractal aggregates, so that we are dealing with 'diffusion limited coalescence' (DLC) [28,29]. The purpose of this section is to calculate the average particle size as a function of time.

We assume that the coalescence rate in such a process is only limited by the diffusion time – the average time needed for particles to cover the interparticle distance to meet each other – and not by the 'particle fusion' itself. Then the problem is reduced to a diffusion limited second order 'reaction' [30]. Such diffusion limited kinetics were already addressed by von Smoluchowski [31,32], who argued that the observed reaction rate constant for this process reads

$$K = 4\pi D' R', \tag{1}$$

where $D' = D_A + D_B$ is the sum of the diffusion coefficients of the reacting species and $R' = R_A + R_B$ is their interaction radius. In the one-component case of coalescing polymers, species A and B both refer to coalescing polymers and an equation for the polymer concentration c_p as a function of time can be readily written as

$$\frac{dc_p}{dt} = -K_{pp} h c_p^2 = -\frac{8}{3}\frac{k_B T}{\eta} h c_p^2, \tag{2}$$

where K_{pp} is the rate constant for polymer–polymer coalescence. In Eq. (2), $D_p = k_B T/(6\pi\eta R_p)$ is the Stokes–Einstein equation for the diffusion coefficient of a sphere with a radius R_p in a fluid with viscosity η. The subscript 'p' refers to 'polymer'. The factor h equals the probability that a collision leads to a coalescence event. We assume $h = 1$ in the absence of surfactant. The coalescence time scale immediately follows from (2)

$$\tau_{cls} = \frac{3}{8 c_{p0}} \frac{\eta}{k_B T}. \tag{3}$$

Since we are dealing with a coalescence process, there is a direct relation between particle mass and particle radius R_p via the mass conservation law in the form

$$c_p(t) R_p^3(t) = c_{p0} R_{p0}^3.$$

Here, R_{p0} and c_{p0} are the size and the number concentration of the polymer particles immediately after mixing took place. The solvent is assumed to be poor enough not to penetrate inside the polymer particles, so $m = 4\pi\rho R_{p0}^3 c_{p0} V/3$. When a certain mass m of a polymer with density ρ has been initially 'suspended' in a volume V, Eq. (2) can be rewritten in terms of the average polymer particle radius

$$\frac{dR_p(t)}{dt} = \frac{2}{3\pi}\frac{k_B T}{\eta}\frac{m}{\rho V}\frac{1}{R_p^2(t)} \tag{4}$$

leading to the solution

$$R_p^3(t) = R_{p0}^3 + \frac{2}{\pi}\frac{k_B T}{\eta}\frac{m}{\rho V} t, \tag{5}$$

or

$$R_p = R_{p0}\left(1 + \frac{t}{\tau_{cls}}\right)^{1/3}, \tag{6}$$

Here R_{p0} is the initial size of the polymer particles, i.e. the size just after the mixing step has been completed. We have neglected the size distribution and derived an equation for the mass averaged radius, $\langle R_p^3 \rangle^{1/3}$. Note that the typical values of the coalescence time τ_{cls} in Eq. (6) are in the ms range.

In order to quantify the time scale τ_{cls} involved, let us take an example with the following numerical values of the parameters: polymer mass $m = 10$ mg with density of approximately $\rho \sim 1$ g/cm^3 is initially suspended in $V = 10$ mL of water with viscosity $\eta \sim 1$ mPa s

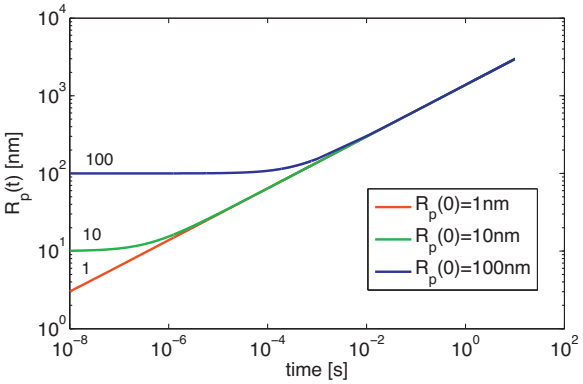

Fig. 2. Size evolution after a quench of Brownian polymer chains in a poor solvent for different initial polymer particle sizes.

at $T = 300$ K. After substituting the numerical values in Eq. (5), we obtain

$$R_p^3(t) = R_{p0}^3 + 2.6 \times 10^6 (\mathrm{nm}^3/\mathrm{s}) \cdot t \quad [\mathrm{s}].$$

The resulting time evolution of the particle size $R_p(t)$ is depicted in Fig. 2 for different initial values of the polymer particle size. Clearly, the initial radius is important only at the very early stages of evolution. Beyond the initial stage a quite universal behavior is observed where the size is solely governed by the mobility and the total amount of polymer. It is also apparent that the coalescence times involved are in the subsecond region. Indeed, it is observed that when one starts with an optically clear suspension, $R_{p0} \lesssim 100$ nm, within less than a second the suspension will become turbid, $R_p(1\ \mathrm{s}) \sim 1\ \mu\mathrm{m}$.

One more important feature of Eq. (5), also reflected in Fig. 2, is that the upper particle size is unbound. In other words, the polymer particles will continue to coalesce until one big (in terms of the current model, big means infinite) particle is formed. This is indeed, what one should expect for a phase separation process in a thermodynamic limit. The situation will dramatically change in the presence of surfactant as explained in the following section.

2.2. Coalescence in the presence of surfactant

Based on the above consideration, a qualitative picture about polymer coalescence *in the presence of surfactant* also emerges. Parallel to coalescence of polymer particles, surfactant adsorption on the polymer particles takes place. Although 'hairy-particle' interaction [33] is quite a complex topic in itself, one point is clear: a surfactant layer on the particle surface hinders coalescence because two densely covered particles cannot approach closely enough to fuse. Steric repulsion between (polymeric) surfactants then leads to a repulsive interaction between two polymer particles.

Thus, in the early stages of the process, polymer particles are 'bald' and easily fuse leading to coarser particles (h is 1 is Eq. (2)). At the same time, the polymer droplets get covered by surfactant and above a certain degree of surfactant surface coverage the coalescence process slows down and stops when the surfaces get saturated with surfactant. This final state leads to a finite polymer particle size, which is purely kinetically determined.

To develop a simple quantitative theoretical model, we make use of the following assumptions:

1. The solvent in the big vessel in Fig. 1 is good for the surfactant molecules (in fact, the surfactant is also a polymer in our experiments). We shall neglect surfactant micellization by assuming that the surfactant molecules present in surfactant micelles behave similarly to the dissolved ones, at least in what concerns their agglomeration with polymeric NPs.
2. Polymer particles and surfactant molecules are both subject to Brownian motion.
3. There is a strong favorable interaction between the polymer and the surfactant. So, when a polymer particle and a surfactant molecule meet, the surfactant 'sticks' to the surface and never desorbs.
4. Polymer particles coalesce when they meet each other, unless they are 'protected' by the surfactant molecules (we shall elucidate this assumption more further on). There is no particle break up.
5. Each surfactant molecule occupies some fixed surface area a^2 when adsorbed. Thus, for a given polymer particle with radius R_p only a limited number of surfactant molecules, $4\pi R_p^2/a^2$, can adsorb on its surface.
6. We use the mean-field continuum approximation.

In what follows, the surfactant effect will be incorporated in the coalescence model of Section 2.1.

2.2.1. Smoluchowski's reaction rate

Now, as we have two 'reacting' species, the reaction rates for a polymer–polymer and polymer–surfactant reactions have to be determined. The expression for the polymer–polymer rate constant remains unchanged [see Eq. (2)] and a similar expression for the polymer–surfactant case can be written [10,11]

$$K_{ps} = 4\pi(D_p + D_s)(R_p + R_s), \tag{7}$$

where K_{ps} is the rate constant that describes surfactant to polymer adsorption. Here R_s is the radius of gyration of the surfactant in solution and the diffusion coefficients are calculated according to the Stokes–Einstein laws

$$D_p = \frac{k_B T}{6\pi\eta R_p} \quad \text{and} \quad D_s = \frac{k_B T}{6\pi\eta R_s} \tag{8}$$

To be precise, using the Zimm expression [34] for the diffusion coefficient of the surfactant molecules in the solvent would be more appropriate. However, it differs from Eq. (8) only by a numerical prefactor, which is not important given the level of accuracy of the present model.

2.2.2. Surfactant concentration

An equation for the concentration of the unadsorbed *free* surfactant molecules can be written using the rate constant from Eq. (7)

$$\begin{aligned} \frac{dc_s^{\mathrm{free}}}{dt} &= -K_{ps} h_s c_s^{\mathrm{free}} c_p \\ &= -\frac{2}{3}\frac{k_B T}{\eta}\left(\frac{1}{R_p} + \frac{1}{R_s}\right)\left(R_p + R_s\right) h_s c_s^{\mathrm{free}} c_p. \end{aligned} \tag{9}$$

The factor h_s appearing in (9) expresses a probability for a surfactant molecule to adsorb upon encountering a polymer particle and is analogous to the factor h in Eq. (2) (for more details see [30]). An interesting observation from Eqs. (9) and (2) is that $\tau_{\mathrm{pro}} \sim \tau_{\mathrm{cls}}$ and, hence, the collision rate of the polymer particles and their protection by the surfactant go at approximately the same pace.

2.2.3. Influence of surfactant on the coalescence rate

Kinetic equations (2) and (9) could be readily solved if the functions h and h_s were specified, which we will do next. Let us first address the probability of particle fusion upon encounter h. The surfactant adsorbed on the particle surface influences h, as it reduces the probability of a coalescence event to occur. Hence, h is a function

of the fraction of the particle surface protected by the surfactant, $h \equiv h\{n(t)a^2/4\pi R_p^2(t)\}$, where $n(t)$ denotes the average number of surfactant molecules adsorbed on a polymer particle with radius R_p at time t, each surfactant molecule covering a surface area a^2.

Computing the exact form of $h(\cdot)$ can be quite involved [35], although it is clear that $h(0) \simeq 1$ and $h(1) \simeq 0$. As a simple approximation we assume h and h_s are the same. Such a choice does not change the scaling of the most relevant quantities but implies that the coalescence process is hindered by surfactant adsorption, and stops abruptly at full coverage when $n = 4\pi R_p^2/a^2$. Hence the coalescence probability is slowed down as the surfactant adsorption increases. It will follow that the exact form of h and h_s do not influence the final result when these functions are identical. It then also follows the coalescence of particles continues until the particles are saturated with the surfactant.

2.2.4. Final set of equations and solution

Let us recapitulate the theoretical model so far. Based on the considerations above, we have arrived at a set of two equations. One equation describes the evolution of the number concentration of the polymer particles c_p during coalescence via Eq. (2) and the other quantifies the free surfactant concentration c_s^{free} given by Eq. (9). For further consideration, it is convenient to recast the expressions in terms of the particle size $R_p = R_{p0}(c_{p0}/c_p)^{1/3}$ and the concentration of the attached surfactant molecules $c_s^{\text{att}} = c_{s0} - c_s^{\text{free}}$:

$$\frac{dR_p}{dt} = \frac{8}{9}\frac{k_BT}{\eta}h(x)\frac{R_{p0}^3 c_{p0}}{R_p^2}, \tag{10}$$

$$\frac{dc_s^{\text{att}}}{dt} = \frac{2}{3}\frac{k_BT}{\eta}\frac{(R_p+R_s)^2}{R_pR_s}h_s(x)(c_{s0}-c_s^{\text{att}})c_p, \tag{11}$$

where $x = na^2/(4\pi R_p^2) = (a^2R_p/R_{p0}^3)(c_s^{\text{att}}/c_{p0})$. The set is completed by the initial conditions $c_s^{\text{att}}(0) = 0$ and $R_p(0) = R_{p0}$.

Solving Eqs. (10) and (11) simultaneously yields the time evolution of the particle size. However, we are interested in the final size of the polymer particles only. Upon dividing Eq. (11) by Eq. (10) and assuming identical functional forms for h and h_s, we arrive at

$$\frac{dc_s^{\text{att}}}{dR_p} = \frac{3}{4}\frac{(R_p+R_s)^2}{R_p^2R_s}(c_{s0}-c_s^{\text{att}}), \tag{11a}$$

$$\frac{a^2R_p}{R_{p0}^3}\frac{c_s^{\text{att}}}{c_{p0}} \le 1, \tag{11b}$$

where an extra inequality is added to the differential equation to fulfill the boundary conditions imposed by the functions h and h_s.

Eq. (11a), (11b) has a simple solution

$$c_s^{\text{att}}(t) = c_{s0}\left\{1 - e^{-\frac{3}{4}\left(\ln\frac{R_p(t)}{R_{p0}} + \frac{R_p(t)-R_{p0}}{R_s} - \frac{R_s}{R_p(t)} + \frac{R_s}{R_{p0}}\right)}\right\}. \tag{12}$$

Enforcing the extra condition of Eq. (11a), (11b) onto Eq. (12) leads to the inequality

$$1 - \exp\left\{-\frac{3}{4}\left[\ln\zeta(t) + \alpha(\zeta(t)-1) + \frac{1}{\alpha}\left(1 - \frac{1}{\zeta(t)}\right)\right]\right\} \le \frac{\kappa}{\zeta(t)}, \tag{13}$$

where some dimensionless quantities have been introduced: $\zeta(t) = R_p(t)/R_{p0}$ is the dimensionless radius of the polymer particles, $\alpha = R_{p0}/R_s$ is the ratio between the initial polymer particle size and the gyration radius of the surfactant molecules, and $\kappa = 4\pi R_{p0}^2 c_{p0}/(a^2 c_{s0})$ is the ratio of the total initial surface area of the polymer particles and the maximum area surfactant molecules can occupy and block.

It can be shown that the largest value of ζ fulfilling inequality (13) corresponds to the equal sign. Hence, solving the corresponding transcendental equation for ζ gives the final particle size. Although Eq. (13) cannot be solved analytically in the general case, explicit solutions can be derived for the final particle size in the asymptotic limit of excess surfactant, $\kappa \ll 1$,

$$R_p^{\text{end}} = R_{p0}\left(1 + \frac{\kappa}{3/4 + \alpha + \alpha^{-1}}\right). \tag{14}$$

If surfactant is scarce, $\kappa \gg 1$, an even simpler analytical formula for the end particle size $R_p^{\text{end}} \equiv \zeta R_{p0}$ can be found:

$$R_p^{\text{end}} = R_{p0}\kappa. \tag{15}$$

The approximate solutions of Eqs. (14) and (15) are surprisingly close to the exact one, as shown in Fig. 3(a), where the asymptotic limits are compared to the numerical results of Eq. (13). It is also interesting to point out that the solution is not very sensitive to the variations in α, the ratio between the initial polymer particle size and the gyration radius of surfactant. Indeed, as Fig. 3(b) shows, only slight variations in the end size values can be observed even if α is changed by two orders of magnitude. The interpolation

$$R_p^{\text{end}} = R_{p0}(1+\kappa) \tag{16}$$

smoothly connects the above asympotic limits and actually describes the numerical results that can be obtained from Eq. (13).

The fact that $\tau_{\text{cls}} \sim \tau_{\text{pro}}$, as pointed out above, implies that the final NP size is independent of the mobility of polymer or surfactant molecules. In the 'fast mixing' limit ($\tau_{\text{mix}} \ll \tau_{\text{cls}}$) the final size depends mainly on the surfactant concentration.

2.2.5. 'Slow mixing' limit

There is also another limit, $\tau_{\text{mix}} \ge \tau_{\text{cls}}$, which is characterized by fast particle coalescence on the time scale shorter than the typical mixing time followed by stabilization of the NPs, thereby setting their final size, at times $t \ge \tau_{\text{mix}}$. At the onset of the coarsening process, the polymers are present as isolated chains in a good solvent. As the solvent quality steeply drops the polymers collapse instantaneously. Subsequent collision of collapsed chains leads to coalescence following the kinetics prescribed by Eq. (10) with $h \equiv 1$. At this stage ($t < \tau_{\text{mix}}$) the surfactants cannot yet adsorb onto the polymer droplets. After full mixing ($t \simeq \tau_{\text{mix}}$), the particle size has evolved to

$$R_{mix} \simeq R_{p0}(1 + \tau_{mix}/\tau_{cls})^{1/3}$$

as follows from Eq. (6). At longer times, $t > \tau_{\text{mix}}$, there is sufficient time for the surfactant to adsorb onto the surface of the coalescing

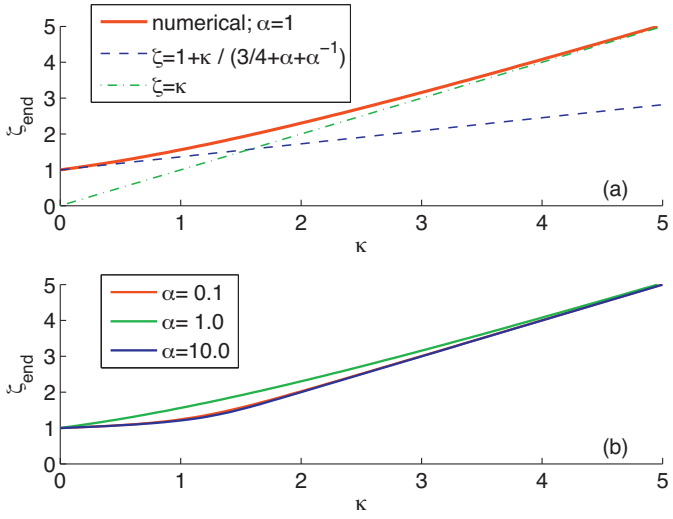

Fig. 3. (a) Comparison between the exact (numerical) solution of Eq. (13) and the approximation of Eq. (14) for $\alpha = 1$. (b) Sensitivity of the solution of the approximate Eq. (14) to the parameter α.

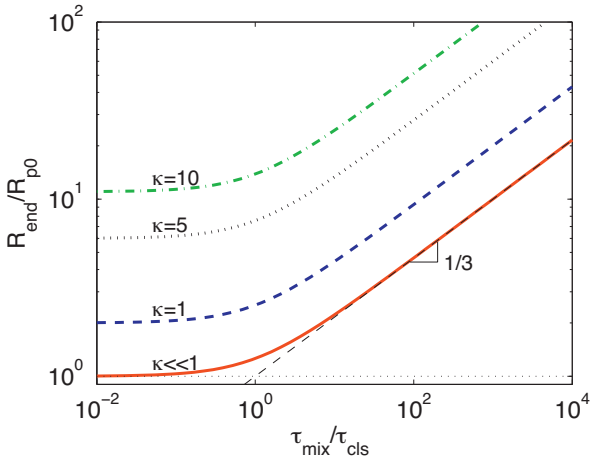

Fig. 4. Particle size as a function of the ratio between mixing and coalescence times for various amounts of surfactants present expressed via κ.

polymer-rich particles. As a result the system then has arrived at a well mixed state and its kinetics obeys the set of Eqs. (10) and (11) as discussed above, with the constraint that R_{mix} must be used as the 'initial' particle size in Eq. (16). This two-step process leads to a final expression for the polymer particle radius in a kinetically frozen state

$$R_p^{end} = R_{p0}(1+\kappa)\left(1+\frac{\tau_{mix}}{\tau_{cls}}\right)^{1/3}. \quad (17)$$

which is depicted in Fig. 4. In Eq. (17) we have used a simple interpolation $(1+\kappa)R_{p0}$ of Eq. (16) for the size after mixing.

The final particle radius (17) is characterized by a plateau at small τ_{mix}/τ_{cls}, where the NP diameter is independent of mixing or encounter and coalescence time and is totally governed by the surfactant concentration (parameter κ) with the smallest particles obtained for large excess of surfactant ($\kappa \ll 1$). The other regime, $\tau_{mix}/\tau_{cls} > 1$, shows a typical 1/3 power law behavior and is dominated by the mixing efficiency. This power law follows from the limit of large τ_{mix} in Eq. (17),

$$R_p^{end} = R_{p0}(1+\kappa)\left(\frac{\tau_{mix}}{\tau_{cls}}\right)^{1/3}.$$

In the practical case of small κ and large τ_{mix} this provides the scaling result

$$R_p^{end} \sim (c_{p0}\tau_{mix})^{1/3}, \quad (18)$$

where we used Eq. (3) for τ_{cls}.

2.3. Implications of the model for experiments

Let us first recapitulate the qualitative model behind the calculation presented so far. The nanoprecipitation can be divided into two important stages: the mixing shown in Fig. 1(b) and the polymer/surfactant diffusion shown in Fig. 1(c) and (d). Clearly, such a division is a bit artificial as there is no clear border between the mixing and the diffusion 'regimes', but we will use it for the sake of simplicity.

At the very beginning of the mixing the polymer 'particles' have the size of a single swollen polymer coil because the polymer is initially dissolved in a good solvent. As soon as the individual polymer chains are solvated by the poor solvent, they collapse to the size of R_{p0} and start coalescing with each other as they are yet not mixed well with the aqueous surfactant solution. When the time τ_{mix} is elapsed, acetone and water are mixed and also some coalescence has taken place leading to the particle size R_{mix}.

Further coalescence is accompanied by protection of the polymer particles by surfactant. As in the experimentally relevant regime there is a large excess of surfactant, $\kappa \ll 1$, the final particle size R_p^{end} is expected to be close to the size at the beginning of the diffusion driven coalescence process, $R_p^{end} \simeq R_{mix} \simeq R_{p0}(1+\tau_{mix}/\tau_{cls})^{1/3}$. Thus, the final polymer particle size in a typical experimental situation is mainly determined by the coalescence during the mixing process and not by the stage after mixing has been completed. The coalescence time expressed via experimentally measurable quantities reads

$$\tau_{cls} = \frac{3}{8}\frac{\eta}{k_B T}\frac{M_p}{N_A c_{mp}} \quad (19)$$

M_p is the polymer molar mass, N_A is the Avogadro's constant, and c_{mp} is the *mass* concentration of polymer in solution. We have used here the initial polymer particle size $R_{p0} = (3M_p/(4\pi N_A \rho))^{1/3}$, where ρ is the polymer density.

The final particle size is plotted in Fig. 4 as a function of the mixing and the coalescence times. Two regimes can be distinguished in Fig. 4: one for large and one for small ratios τ_{mix}/τ_{cls}. For very fast mixing, $\tau_{mix}/\tau_{cls} \ll 1$, the final radius is of the order of R_{p0} and does not depend on τ_{cls}. Hence, the final particle size does not depend on the polymer concentration in the limit of very fast mixing, but does depend on the molar mass. In the slow mixing regime, $\tau_{mix}/\tau_{cls} > 1$, a power law scaling of the final polymer particle size with an exponent of 1/3 is predicted: $R_p^{end} \sim R_{p0}(\tau_{mix}/\tau_{cls})^{1/3} \sim \tau_{mix}^{1/3}[k_B T c_{mp}/(\eta\rho)]^{1/3}$. Here the final size will increase if τ_{cls} is decreased, e.g. due to higher concentration.

Let us finally summarize the conclusions and the theoretically predicted trends, which can be used to control the particle size experimentally:

1 Under the currently used experimental conditions – excess of surfactant – the particle size at the end of the mixing phase determines the final size of the surfactant stabilized NPs. The particles are stabilized by the surfactant corona and the system is in a kinetically frozen state.
2 In the slow mixing regime, the size of the micelles formed is proportional to the polymer concentration to power 1/3: $R_p^{end} \sim c_{mp}^{1/3}$ [10,11]. So, the lower the concentration, the smaller particles can be formed.
3 Fast mixing is essential: smaller particles are obtained when τ_{mix} is reduced.
4 In case of relatively slow mixing, as typically encountered in experiment, the end size is independent of the initial size of the polymer particles. This implies, that the final size will be insensitive to the molar mass of the polymer.
5 There is no explicit dependence on the molar mass of the surfactants. However, the mixing time will probably increase if higher molar mass of the surfactant is added at constant surfactant concentration ϕ. Indeed, the (shear) viscosity of the aqueous solution of surfactant (in our experiments PVA) will scale as $\eta_m(1+\phi[\eta])$, with medium viscosity η_m and where the intrinsic viscosity is proportional to the molar mass $[\eta] \sim M_s^{0.8}$ (we have used Zimm model in a good solvent, [34]). A higher shear viscosity of the solution implies longer mixing times and, hence, larger NPs.
6 Another parameter, which possibly plays a role, is the temperature. As many model parameters (weakly) depend on it, explicitly and implicitly, it is hardly possible to elucidate what the exact effect of the temperature should be. Apparently, the higher the temperature, the lower the coalescence time τ_{cls}, see Eq. (19). But also the mixing time τ_{mix} will probably be decreasing upon temperature rise. Although it is hard to predict what the net effect

on the ratio τ_{mix}/τ_{cls} will be, we mention it as a tool to adjust the particle size to a limited degree.

3. Materials and methods

3.1. Materials

Polycaprolactone (PCL) of different molar masses (CAPA 2203; 2 kDa, 2403; 4 kDa, 2803; 8 kDa, 6250; 25 kDa, 6400; 37 kDa, 6500; 50 kDa and 6800; 80 kDa) were purchased from Solvay (Oudenaarde, Belgium). Poly-(lactic-co-glycolic) acid (PLGA; 1/1 molecular ratio for lactic and glycolic acid) 20 kDa was purchased from Boehringer Ingelheim (Ingelheim am Rhein, Germany). Acetone and Pluronic F127 (NF prill polaxamer 407) were purchased from BASF (Bayern, Germany). Polyvinylalcohol (PVA) of different molar masses (13–23 kDa, 31–50 kDa and 85–124 kDa; all three with a hydrolyzation percentage of 87–89% and 9–11 kDa 80% hydrolyzed) were purchased from Sigma (St. Louis, USA). Rapamycin was obtained from Oscar Tropitzsch (Germany).

3.2. Particle size analysis

3.2.1. Dynamic light scattering

The final hydrodynamic diameter of the particles was determined by Dynamic Light Scattering (DLS) (Zetasizer Nano ZS, Malvern Instruments Ltd., Malvern, UK) at 25 °C at a scattering angle of 173°. Ideally the number of photon counts is large enough to get a good signal to noise ratio and yet small enough to prevent multiple scattering effects. In dynamic light scattering the fluctuations in the scattered intensity are analyzed and the resulting autocorrelation function is related to an averaged diffusion coefficient of the particles that undergo Brownian motion. Via the Stokes–Einstein relation the diffusion coefficient is converted to a hydrodynamic particle size diameter, D_h. We note that this diameter is the z-average of the size distribution. We also report the measured polydispersity index (PdI) that describes the width of the particle size distribution. The polydispersity index is a parameter calculated from the cumulant analysis of the DLS measured intensity autocorrelation function. In the cumulants analysis, a single particle size is assumed and a single exponential fit is applied to the autocorrelation function. All samples were measured as processed (undiluted). Size distributions of the prepared NPs measured with DLS were unimodal.

3.2.2. Cryo-TEM

For a few samples we also studied the size using cryo transmission electron microscopy (cryo-TEM) at the TU Eindhoven in the Netherlands. The aqueous samples were prepared with a vitrification robot from FEI; Vitrobot(tm) Mark III. The used cryo-TEM equipment was a cryoTITAN from FEI, a 300 kV FEG microscope, optimized for both resolution and contrast. Two samples containing particles made of only active ingredient and a combination rapamycin and PLGA were analyzed using cryo-TEM. The first sample was pure rapamycin; 1.00 mL of 60 mg rapamycin/mL acetone. The second sample was a rapamycin and PLGA (20 kDa) (1/1 mass ratio); 15 mg rapamycin and 15 mg of PLGA/mL acetone. The samples were added to an aqueous solution with a volume of 10.00 mL (containing 1 wt%) PVA (9–11 kDa 80% hydrolyzed) according to the nanoprecipitation procedure followed by cryo-TEM and DLS analysis were performed.

3.3. Rheology of PVA solutions

The shear stress of solutions with PVA were measured as a function of shear rate in order to investigate the influence of the viscosity on the NP size. We studied solutions containing three different molar masses of PVA (13–23 kDa, 31–50 kDa and 85–124 kDa; all three with a degree of hydrolysis of 87–89%). The polymer solutions were analyzed at five different weight concentrations (2.50, 1.00, 0.50, 0.25 and 0.10% (wt%)). The viscosity measurement was performed on an Anton Paar MCR 300 Rheometer at 25 °C with a double gap cylinder (DG 26.7). The shear rate was varied between 30 and 300 s^{-1}. At these concentrations the solutions appeared Newtonian.

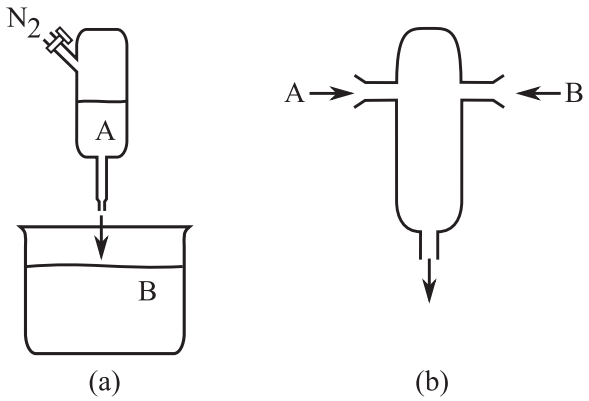

Fig. 5. Scheme of a pressure driven injection device used in Ref. [36] (a) and an impinging jets mixer used in [13] (b). Fluid A is the organic phase comprising solvent, the carrier polymer and the drug, fluid B is an aqueous solution containing (polymeric) surfactant.

3.4. Nanoprecipitation/nanoparticle preparation method

Typically, 25.0 mg of polymer (PCL) was weighed and dissolved in 5.00 mL of acetone resulting in a clear polymer solution after 30 min on an orbital shaker. Prior to the nanoprecipitation process all solutions were filtered over an Acrodisc LC25 mm Syringe filter 0.2 μm PVDF membrane to remove large dust particles. In Fig. 1 the basic nanoprecipitation process setup was sketched. A volume of 1.00 mL of the polymer/acetone solution was added to 10.00 mL of aqueous surfactant (PVA or Pluronic F127) solution with an Eppendorf pipette. The addition with the pipette was carried within 1 s, after which the suspension was manually homogenized by swirling the vial around for 5 s. We will compare our experiments to the proposed theoretical model for diffusion limited coalescence in the slow mixing regime and with data from literature. For the fast mixing regime we will test our theoretically predicted trends against data from literature.

There are various other ways to perform nanoprecipitation. Two of them are depicted in Fig. 5. One will result in slow mixing times [36]. Experiments using an impinging jets mixer allow tuning the mixing time scale as to investigate both the fast and slow mixing time regimes [13]. The results reported in literature will be used to verify our theoretically predicted trends:

- in the slow mixing regime, $\tau_{mix}/\tau_{cls} > 1$, a cube root scaling of the final polymer particle size with polymer concentration is predicted: $R_p^{end} \sim R_{p0}(\tau_{mix}/\tau_{cls})^{1/3} \sim \tau_{mix}^{1/3}[k_B T c_{mp}/(\eta\rho)]^{1/3}$ and thus: $R_p^{end} \sim c_{mp}^{1/3}$,
- in the limit of fast mixing, $\tau_{mix}/\tau_{cls} \ll 1$, the final radius is of the order of R_{p0} and does not depend on τ_{cls}. Hence, the final particle size is expected to be independent of the polymer concentration, but dependent on the molar mass.

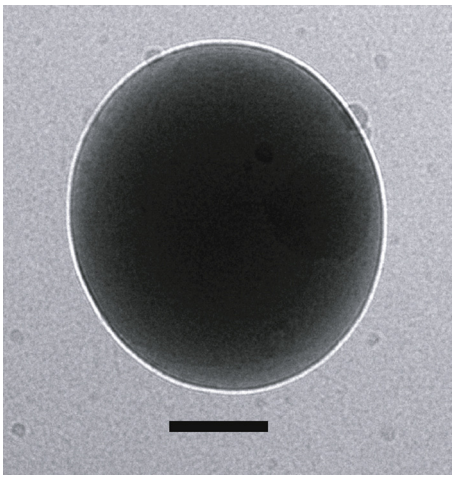

Fig. 6. Cryo-TEM picture of a nanoparticle prepared by nanoprecipitation filled with the drug rapamycin. The scale bar is 100 nm. The dispersion was prepared by adding 1.00 mL acetone containing 60 mg rapamycin to 10.00 mL with 1.00 wt% aqueous solution of 9–11 kDa PVA. (Corresponding DLS results: D_h = 344 nm and PdI = 0.10.)

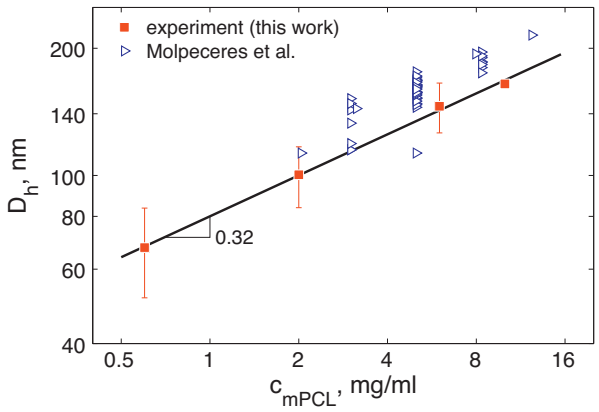

Fig. 8. Polymer concentration dependence of the generated particle size expressed as the hydrodynamic diameter (D_h), measured with DLS. These particles form after adding 1.00 mL of different PCL concentrations (molar mass: 25 kDa) in acetone (mg/mL) to 10.00 mL water containing 1 wt% Pluronic F127 (squares). Each data point results from the average of three measurements. We compare these results to the theoretical scaling relation of Eq. (18) and data from Molpeceres [36] (open triangles).

4. Results and discussion

4.1. Cryo-TEM images of NPs

To illustrate what kinds of particle sizes form after nanoprecipitation using real space analysis we show two (cryo-)TEM pictures. Figs. 6 and 7 depict the cryo-TEM pictures of a pure rapamycin particle and a rapamycin/PLGA (1/1 mass ratio) particle, respectively. The DLS results of the particles are in good agreement with size from the cryo-TEM analysis, see Figs. 6 and 7 and their legends. In Fig. 7 a small gold particle can be seen in the right upper corner, which was added to serve as a reference point to perform tomography, revealing a spherical shape.

4.2. Influence of polymer concentration on size

To validate Eq. (18) we compare its scaling prediction $R_p^{end} \sim c_{mp}^{1/3}$ to our experiments as well as to data available in the literature. In the nanoprecipitation experiments we performed, PCL (CAPA 6250; 25 kDa) has been used as a carrier polymer and Pluronic F127 as a surfactant. 1.00 mL PCL/acetone solution (0.6, 1.0, 6.0 and 10.0 mg PCL (25 kDa)/mL acetone) was quenched in 10.00 mL, 1.00 wt%, Pluronic F127 aqueous solution with an Eppendorf pipette, a device similar to the one depicted in Fig. 5. The hydrodynamic particle diameter D_h has been measured by DLS.

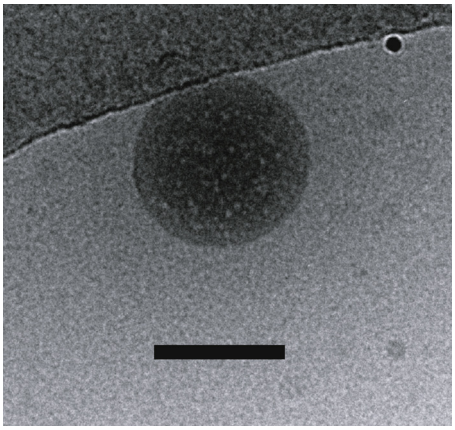

Fig. 7. Cryo-TEM picture of a rapamycin/PLGA nanoprecipitated particle. Scale bar is 100 nm. A volume of 1.00 mL with 15 mg rapamycin and 15 mg PLGA acetone was added to an aqueous solution of 10.00 mL with 1.00 wt% 9–11 kDa PVA. (Results from DLS: D_h = 148 nm and PdI = 0.06.)

As can be seen from Fig. 8, our results compare favorably to the data available in the literature [6] for the same system. As the experiments are performed in the $\tau_{mix} > \tau_{cls}$ regime, the scaling obeys the 1/3 power law as expected. The data presented only cover the $\tau_{mix} > \tau_{cls}$ regime and neither reach a particle size saturation limit at the very fast mixing, $\tau_{mix} < \tau_{cls}$, nor a crossover at $\tau_{mix} \approx \tau_{cls}$. The spread on the data of Molpeceres et al. can be explained by experimental and analytical standard deviation since the spread is equal to the error bars in our experiments, see Fig. 8. Our experiments were repeated on different dates using freshly prepared solutions. The scaling $R_p^{end} \sim c_{mp}^{1/3}$ has been found and confirmed earlier by Cabane and co-workers [10,11] for various systems such as cholesteryl acetate molecules dispersed in water in the presence of the block copolymer polystyrene–polyoxyethylene as surfactant or hexadecane molecules precipitated in water with exthoxylated fatty acids as surfactants. The physical picture thus also holds for precipitating hydrophobic molecules instead of hydrophobic polymers.

One may wonder how polymer polydispersity affects the final particle size (distribution). This was considered by Whitesides and Ross [19] in a numerical study. They found that the final particle size is quite independent of the starting distribution. Hence it seems that the final particle size is not sensitive to the initial polydispersity.

4.3. NP size dependence on polymer molar mass

In case of relatively slow mixing, typically encountered in our experiments, there should be no dependence between final particle size and the molar mass of the polymer as follows from Eq. (17). In order to verify this the influence of using PCL polymers with different molar masses (2, 4, 8, 25, 37, 50 and 80 kDa) on particle size was studied. The PCL polymers were dissolved at equal concentrations in acetone (5 mg PCL/mL acetone). A volume of 1.00 mL of the different polymer/acetone solutions were added to 10.00 mL aqueous solution containing 1.00 wt% Pluronic 127 F following the nanoprecipitation procedure. All experiments were done in triplicate after which a DLS analysis was performed.

In Fig. 9 we plotted the measured particle size as a function of the molar mass of the hydrophobic polymer. It is clear that changing

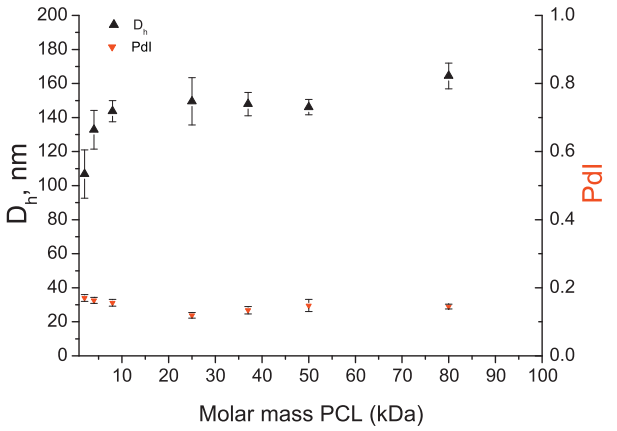

Fig. 9. Hydrodynamic diameter (D_h) and PdI results (triplicates) as a function of the molar mass of PCL at fixed concentration. Samples were made by adding 1.00 mL acetone with 5 mg/mL PCL of different molar masses to 10.00 mL water containing 1 wt% Pluronic F127.

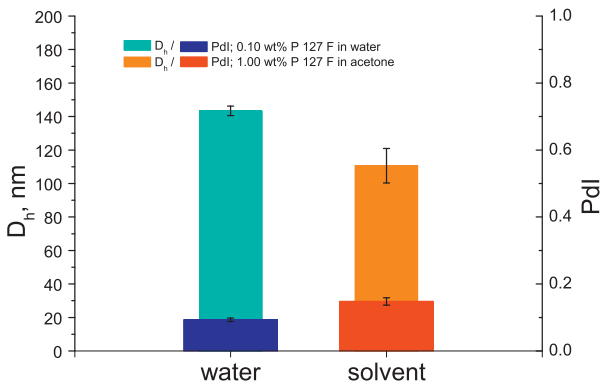

Fig. 10. Effect of surfactant present in the organic phase or the aqueous phase. Averaged values for size and polydispersity D_h and PdI from triplicates. Results were obtained by adding 1.00 mL acetone with 5 mg PCL (25 kDa)to an aqueous solution with a volume of 10.00 mL. The surfactant, Pluronic F127, is either in the water phase (indicated by 'water') or in the acetone phase ('solvent'). The overall Pluronic F127 concentration in the final mixture is 0.1 wt%.

the molar mass hardly affects the final particle size under the same experimental conditions. The particle size ranges between 130 nm and 150 nm, which can be explained by a slightly different viscosity of the polymer/acetone solutions. The lower molar masses hardly influence the viscosity of the polymer/acetone solution while the higher molar masses (80 kDa) of PCL have a more distinct effect on the viscosity of the polymer/acetone solution. The difference between the values for the viscosity of these solutions hardly alters the mixing times and therefore only modifies the final particle size to a small degree. Further the data for molar masses (below 10 kDa) could reflect slightly smaller sizes because the solubility starts to increase a bit for lower molar mass.

4.4. Influence of mixing time on particle size

The end particle size is governed by two relevant time scales; the mixing and the coalescence time. To assess the influence of the mixing time while maintaining the same experimental conditions only the phase containing the surfactant was changed. In a first experiment the surfactant was dissolved in the water phase (0.10 wt% Pluronic F127 in water). A volume of 1.00 mL acetone/polymer-solution (5 mg PCL (25 kDa)/mL acetone) was added to 10.00 mL 1.00 wt% Pluronic F127 solution, according to the nanoprecipitation procedure. In a second experiment the surfactant was co-dissolved with the polymer in the acetone phase (1.00 wt% Pluronic F127 + 5 mg PCL (25 kDa)/mL acetone. Then 1.00 mL surfactant/polymer/acetone solution was added to 10.00 mL Milli Q water according to the nanoprecipitation procedure. Both experiments were performed in triplicate followed by a DLS analysis. The difference of surfactant concentration in the acetone phase (1.0 wt%) and the surfactant in the water phase (0.10 wt%) was chosen such that the final surfactant concentration was the same for both experiments.

The presence of the surfactant in the aqueous phase or in the solvent (acetone) phase together with the hydrophobic polymer should have a distinct influence on the final particle size. This is explained by the mixing time which is decreased in the latter case. Since the hydrophobic polymer and surfactant are dissolved in the same phase the mixing time decreases resulting in a smaller final particle size. It is the diffusion time of the surfactant molecules to the coalescing droplets which is mainly decreased, resulting in a smaller final particle size, as can be seen in Fig. 10.

In case of relatively slow mixing, typically encountered in our experiments, there should be no dependence between final particle size and the molar mass of the polymer. To assess the dependency of the mixing time on the molar mass and the viscosity of the used surfactant solutions different molar masses of PVA (13–23, 31–50 and 85–124 kDa; similar degree of hydrolyzation of 87–89%) dissolved in water at different concentrations (0.10, 0.25, 0.50, 1.00 and 2.50 wt% of surfactant in water). The viscosity of these solutions was measured in order to grasp the influence of both the molar mass of the surfactant and the viscosity of the solutions in relation to the final particle size. In all experiments 5 mg PCL (25 kDa)/mL acetone was added to 10.00 mL of the different PVA/water solutions. Also here each experiment was done in triplicate after which DLS analysis was performed.

Besides a comparison of the size between these two extreme cases above we confront our theoretical predictions to the results obtained by Johnson and Prud'homme [13] who have carefully varied τ_{mix}. They studied a somewhat different system comprising a methanol solution of an amphiphilic diblock copolymer (polybutylacrylate-b-polyacrylic acid) quenched in water. By using a highly efficient impinging jet mixer, see Fig. 5, Johnson and Prud'homme [13] succeeded in covering a very broad range of mixing times and observed various regimes. Their original measured data for the hydrodynamic diameters of the particles formed as a function of the mixing time are shown in Fig. 11. The coalescence in a dispersion containing diblock copolymers must obey kinetics very similar to the one described by Eq. (1) and, thus, yield scaling Eq. (17) for the NP size. This implies that a master curve must be obtained in Fig. 11 if one shifts the data along the abscissa by

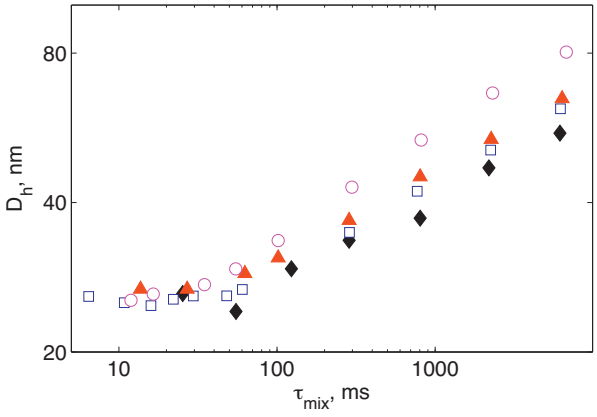

Fig. 11. The original data from Johnson and Prud'homme [13].

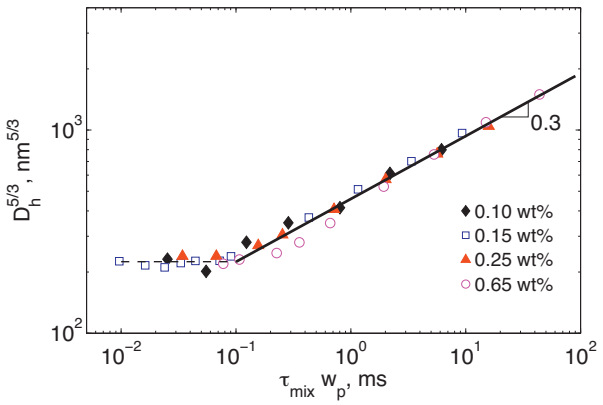

Fig. 12. Master curve of the size of the core of the diblock copolymer NPs vs the rescaled mixing time, following the scaling predicted by Eq. (17), original data from Johnson and Prud'homme [13]. Note that we use the quantity w_p as polymer concentration on the abscissa. This is the weight fraction (dimensionless) which is directly linked to the mass concentration c_{mp} via the density. The quantity $w_p\tau_{mix}$ is proportional to $c_{p0}\tau_{mix}$ in Eq (18).

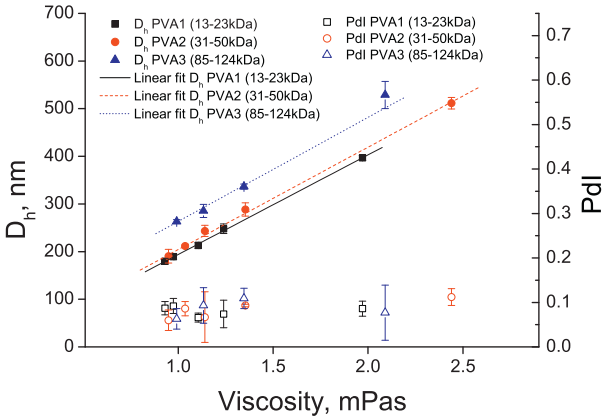

Fig. 13. Linear dependence of the final particle size (D_h) and PdI on the surfactant molar mass and surfactant solution viscosity.

the polymer mass fraction w_p. Moreover, a typical diameter scaling $(\tau_{mix}w_p)^{1/3}$ is expected to be observed at long mixing times.

One important difference between the concentration dependence of the size predicted by our theory and the work of Johnson and Prud'homme [13] is the fact that our Eq. (17) does not take into account the size of the surfactant layer on top of a NP. Indeed, such an approximation certainly holds in case of a polymeric surfactant. In case of diblock copolymers, however, the size of the hydrophilic corona surrounding the hydrophobic core cannot be neglected. To compute a hydrophobic core diameter from a hydrodynamic diameter of a copolymer micelle, we use the theoretical result of Daoud and Cotton [37] that the latter scales as a power 1/5 of the micelle mass. As the core of a micelle consists almost solely of the hydrophobic polymer segments, the core size scales as a power 1/3 of the mass, yielding $R_{core} \propto D_h^{5/3}$.

The data obtained by Johnson and Prud'homme [13], see Fig. 11, are redrawn in $D_h^{5/3}$ versus $\tau_{mix}c_p$ coordinates in Fig. 12. Indeed the data follow a master curve obeying Eq. (17): it is characterized by a typical $(\tau_{mix}/\tau_{cls})^{1/3}$ scaling at long mixing times and shows a plateau in the fast mixing regime, exactly as the theory predicts. Our theoretical results hence rationalize the findings on the influence of the mixing time by Johnson and Prud'homme. Note, that the NP size in Fig. 12 is completely determined by the kinetics and is not related to the equilibrium diblock copolymer micelle size. Indeed the latter would depend solely on the molar mass, composition, and solvent quality, whereas the NP size is a strong function of concentration. Although the NP system is not in thermodynamic equilibrium, it is long-lived. As an X-ray study on a somewhat different diblock copolymer system [38] shows, micellization of copolymers is a process consisting of two stages. The first rapid stage is totally controlled by kinetics and leads to the NP formation described in the present work. The second process, that is several orders of magnitude slower, drives the NP system to thermodynamic equilibrium. Studying this slow process is outside of the scope of the present work.

4.5. Surfactant molar mass influence

To assess the dependency of the mixing time on the molar mass and the viscosity of the used surfactant solutions the effect of different molar masses of PVA (13–23, 31–50 and 85–124 kDa with similar degree of hydrolyzation of 87–89%) was studied. These PVA samples were dissolved in water at different concentrations (0.10, 0.25, 0.50, 1.00 and 2.50 wt% of surfactant in water). The viscosity of these solutions was measured in order to assess the influence of both the molar mass of the surfactant and the viscosity of the solutions in relation to the final particle size. In all experiments 5 mg PCL (25 kDa)/mL acetone was added to 10.00 mL of the different PVA/water solutions. Also here each experiment was done in triplicate, followed by dynamic light scattering measurements of these samples.

In Fig. 13 the size obtained after nanoprecipitation as measured using DLS is plotted as a function of the solution viscosity when using PVA varying in molar mass. It is shown that the size is linearly dependent on the viscosity of the surfactant solution and slightly increases with the molar mass of the used surfactant. Based on our model, the influence of the surfactant molar mass can be explained qualitatively. Let us first focus on how particle size depends on viscosity. As the experiments are performed in excess of surfactant, one expects the final particle size scaling $R_p^{end} \sim R_{p0}(\tau_{mix}/\tau_{cls})^{1/3} \sim \tau_{mix}^{1/3}[k_BTc_{mp}/(\eta\rho)]^{1/3}$. Note that the viscosity of the medium here refers to a surfactant-free environment where the coalescence of polymer droplets takes place before surfactant penetrates into it at $t > \tau_{mix}$. Hence, η in the last form hardly depends on surfactant properties. The mixing time τ_{mix}, on the other hand, is expected to be determined by the viscosity of the surfactant solution in the vessel B in Fig. 5(a): the higher the viscosity the slower the mixing. Hence, based on the theoretical picture, one expects the final particle size to increase with increasing surfactant solution viscosity.

Secondly, we concentrate on the influence of the molar mass of the surfactants used. In Fig. 13 it can be observed that the final size is larger for a higher molar mass surfactant at fixed viscosity of the continuous phase. The change can be rationalized easily. The final size depends on κ according to Eq. (16). The quantity κ in turn (see text below Eq. (13)) is inversely proportional to c_{s0}, the initial concentration of free surfactant. The viscosity increases with molar mass and concentration of the free surfactant. Hence at fixed viscosity the concentration of higher molar mass surfactants is smaller. So at a fixed bulk viscosity the higher molar mass data correspond to smaller surfactant concentrations leading to a higher value of κ and hence, via Eq. (16), to a larger value for the final particle size. This holds for all measured data points in Fig. 13.

It therefore seems the influence of the molar mass of the surfactant and the viscosity of the surfactant solution is twofold. Firstly, a higher viscosity will result in a longer mixing time which increases the final particle size upon mixing. Secondly, using a higher molar mass of the surfactant will probably increase the adsorption time scale of the surfactant molecules to some degree. This might lead to the observed slight increase of the final particle size.

Finally, we remark that we assumed that the equilibrium between free surfactant and surfactants in the micelles is faster than the typical coalescence time scale. From Eq. (3) it follows that for a typical initial polymer concentration of 5 mg/mL for PCL with molar mass of 25 kDa the time scale for coalescence is of the order of 1 s. The typical time scale for block copolymers exchanging in a micelle is about 1 ms (see Refs. [39,40]). This supports our assumption. Hence we may safely assume there is no effect of the value for the critical micelle concentration.

5. Conclusions

We have studied nanoprecipitation of polymers in a bad solvent in the presence of (polymeric) surfactants. The polymer is first dissolved in a good (organic) solvent, followed by a solvent switch towards a poor solvent environment in the presence of surfactant. The combined experimental and theoretical results on nanoprecipitation demonstrate that diffusion limited coalescence is a mechanism that enables an adequate description of the nanoparticle formation process. Two relevant time scales, the mixing and coalescence times, can be identified and their ratio is shown to be of a critical importance for the size evolution. It is shown that the final particle size is determined mainly by the surfactant concentration in the fast mixing regime. In the case of slow mixing the final particle size is also dependent on the initial concentration of the collapsing and coalescing polymers, and the mixing time. In the slow mixing regime the particle volume scales linearly with mixing time and polymer concentration.

The theoretical model illustrates that the nanoparticle size is predicted to scale in a universal manner; it is predominantly sensitive to the mixing time and the polymer concentration if the surfactant concentration is sufficiently high. The molar mass of the carrier polymer is shown to have little influence. Available experimental data corroborate the predictions of our model and provide a solid framework for tailoring nanoparticles with *a priori* determined size, thus avoiding a laborious experimental trial and error approach.

Acknowledgments

We thank Professor R. Prud'homme for useful discussions and P.H.H. Bomans for performing the cryo-TEM analyses.

References

[1] T. Niwa, H. Takeuchi, T. Hino, N. Kunou, Y. Kawashima, J. Control. Release 25 (1993) 89–98.
[2] According to the IUPAC definition a nanoparticle is a particle of any shape with dimensions in the 1–100 nm range. The method of Niwa et al. allows to make particles in that size range. We note however that it is also possible to make larger particles using this precipitation method.
[3] K.S. Soppimath, T.M. Aminabhavi, A.R. Kulkarni, W.E. Rudzinski, J. Control. Release 70 (2001) 1–20.
[4] J. Panyam, V. Labhasetwar, Adv. Drug Deliv. Rev. 55 (2003) 329–347.
[5] S. Hornig, T. Heinze, C.R. Becer, U.S. Schubert, J. Mater. Chem. 19 (2009) 3838–3840.
[6] S. Galindo-Rodriguez, E. Alleèmann, H. Fessi, E. Doelker, Pharm. Res. 21 (2004) 1428–1439.
[7] T. Kietzke, D. Neher, K. Landfester, R. Montenegro, R. Gütner, U. Scherf, Nat. Mater. 2 (2003) 408–412.
[8] D. Peer, J.M. Karp, S. Hong, O.C. Farokhzad, R. Margalit, R. Langer, Nat. Nanotechnol. 2 (2007) 751–760.
[9] K. Koo, M.S. Huh, I.-C. Sun, S.H. Yuk, K. Choi, K. Kim, I.C. Kwon, Acc. Chem. Res. 44 (2011) 1018–1028.
[10] H. Lannibois, A. Hasmy, R. Botet, O.A. Chariol, B. Cabane, J. Phys. II France 7 (1997) 318–342.
[11] J. Aubry, F. Ganachaud, J.-P. Cohen Addad, B. Cabane, Langmuir 25 (2009) 1970–1979.
[12] K. Roger, R. Botet, B. Cabane, Langmuir 29 (2013) 5689–5700.
[13] B.K. Johnson, R.K. Prud'homme, Phys. Rev. Lett. 91 (2003) 118302.
[14] T. Chen, S.M. D'Addio, M.T. Kennedy, A. Swietlow, I.G. Kevrekidis, A.Z. Panagiotopoulos, R.K. Prud'homme, Nano Lett. 9 (2003) 2218–2222.
[15] Y. Liu, K. Kathan, W. Saad, R.K. Prud'homme, Phys. Rev. Lett. 98 (2007) 036102.
[16] M. Akbulut, P. Ginart, M.E. Gindy, C. Therihault, K.H. Chin, W. Soboyejo, R.K. Prud'homme, Adv. Funct. Matter 19 (2009) 718–725.
[17] D. Horn, J. Rieger, Angew. Chem. Int. Ed. 40 (2001) 4339–4361.
[18] C. Vauthier, K. Bouchemal, Pharm. Res. 26 (2009) 1025–1058.
[19] T.H. Whitesides, D.S. Ross, J. Colloid Interface Sci. 169 (1995) 48–59.
[20] S.J. Marrink, D.P. Tieleman, A.E. Mark, J. Phys. Chem. B 14 (2000) 12165–12173.
[21] T. Chen, A.-P. Hynninen, R.K. Prud'homme, I.G. Kevrekidis, A.Z. Panagiotopoulos, J. Phys. Chem. B 112 (2008) 16357–16366.
[22] J.G.J.L. Lebouille, T. Kockelkoren, L.F.W. Vleugels, R. Tuinier, Micelle compositions and process for the preparation thereof, US Patent 2011/0223206A1 (September 5, 2011).
[23] J.G.J.L. Lebouille, R. Tuinier, L.F.W. Vleugels, M.A. Cohen Stuart, F.A.M. Leermakers, Soft Matter 9 (2013) 7515–7525.
[24] J.G.J.L. Lebouille, L.F.W. Vleugels, A. Dias, F.A.M. Leermakers, M.A. Cohen Stuart, R. Tuinier, Eur. Phys. J. E 36 (2013) 107.
[25] L.G.B. Bremer, T. Van Vliet, P. Walstra, J. Chem. Soc., Farad. Trans. 2 (85) (1989) 3359–3372.
[26] L.G.B. Bremer, B.H. Bijsterbosch, R. Schrijvers, T. Van Vliet, P. Walstra, Colloids Surf. 51 (1990) 159–170.
[27] L.G.B. Bremer, B.H. Bijsterbosch, P. Walstra, T. van Vliet, Adv. Colloid Interface Sci. 46 (1993) 117–128.
[28] D. Ben-Avraham, Phys. Rev. Lett. 81 (1998) 4756.
[29] R. Stepanyan, J.G.J.L. Lebouille, J.J.M. Slot, R. Tuinier, M.A. Cohen Stuart, Phys. Rev. Lett. 109 (2012) 138301.
[30] J. Keizer, Chem. Rev. 87 (1987) 167–180.
[31] M. von Smoluchowski, Kolloid-Z 18 (1916) 48–54.
[32] M. von Smoluchowski, Kolloid-Z 21 (1917) 98–104.
[33] W.B. Russel, D.A. Saville, R. Schowalter, Colloidal Dispersions, Cambridge University Press, Cambridge, 1989.
[34] M. Doi, S. Edwards, The Theory of Polymer Dynamics, Clarendon Press, Oxford, 1986.
[35] G.J. Fleer, M.A. Cohen Stuart, J.M.H.M. Scheutjens, T. Cosgrove, B. Vincent, Polymers at Interfaces, 1st ed., Chapman and Hall, London, 1993.
[36] J. Molpeceres, M. Guzman, M.R. Aberturas, M. Chacon, Y. Kawashima, J. Control. Release 85 (1996) 206–213.
[37] M. Daoud, J.P. Cotton, J. Phys. Paris 43 (1982) 531–538.
[38] R. Lund, L. Willner, M. Monkenbusch, P. Panine, T. Narayanan, J. Colmenero, D. Richter, Phys. Rev. Lett. 102 (2009) 188301.
[39] R. Lund, L. Willner, J. Stellbrink, A. Radulescu, D. Richter, Phys. Rev. B 350 (2004) 909.
[40] R. Lund, L. Willner, D. Richter, Macromolecules 39 (2006) 4566.